# Static and Dynamic Polarizabilities of Conjugated Molecules and Their Cations

**Stanley M. Smith,[†] Alexei N. Markevitch,[‡,§] Dmitri A. Romanov,[§,||] Xiaosong Li,[†] Robert J. Levis,[‡,§] and H. Bernhard Schlegel*[,†,⊥]**

*Department of Chemistry and Institute for Scientific Computing, Wayne State University, Detroit, Michigan 48202, and Departments of Chemistry and Physics, Center for Advanced Photonics Research, Temple University, Philadelphia, Pennsylvania 19122*

*Received: March 14, 2004; In Final Form: September 30, 2004*

Recent advances in nonlinear optics and strong-field chemistry highlight the need for calculated properties of organic molecules and their molecular ions for which no experimental values exist. Both static and frequency-dependent properties are required to understand the optical response of molecules and their ions interacting with laser fields. It is particularly important to understand the dynamics of the optical response of multielectron systems in the near-IR ($\lambda \sim 800$ nm) region, where the majority of strong-field experiments are performed. To this end we used Hartree−Fock (HF) and PBE0 density functional theory to calculate ground-state first-order polarizabilities ($\alpha$) for two series of conjugated organic molecules and their molecular ions: (a) all-trans linear polyenes ranging in size from ethylene ($C_2H_4$) to octadecanonene ($C_{18}H_{20}$) and (b) polyacenes ranging in size from benzene ($C_6H_6$) to tetracene ($C_{18}H_{12}$). The major observed trends are: (i) the well-known nonlinear increase of $\alpha$ with molecular size, (ii) a significant increase of $\alpha$ upon ionization for larger systems, and (iii) for larger ions, the dynamic polarizability at 800 nm is much larger than the static polarizability. We have also compared the HF and PBE0 polarizabilities of the linear polyenes up to octatetraene calculated with second-order Moller−Plesset perturbation theory (MP2) and coupled cluster theory with single and double excitations (CCSD). For neutral molecules the results at the PBE0 and HF levels are very similar and ca. 20% higher than the MP2 and CCSD results. For molecular ions, results at the HF, PBE0, MP2, and CCSD are all very close. We discuss the size scaling and frequency dependence of $\alpha$, and provide simple models that capture the origin of the change in the static and dynamic polarization upon ionization.

## Introduction

Accurate information about optical properties of conjugated molecules is highly desirable because such molecules are used in a variety of technologically important applications. Opto-electronic logical circuits,[1] three-dimensional optical data storage,[2−5] photo dynamic therapy,[6] and biological imaginig[7,8] are just a few of the key applications. One of the most important optical properties of conjugated molecules is their polarizability. The polarizability of conjugated molecules has drawn considerable attention in the past few decades, mostly in the context of linear (or weak-field) excitations.[9−14] Polarizabilities of first, second, and higher orders have been calculated[15] for polyethylene,[16−19] polyacetylene,[18,20−23] polyacenes,[24,25] and polythiophenes[26] as well as for donor−acceptor substituted polymers.[27−30] Static polarizabilities have been calculated using finite field, coupled perturbed Hartree−Fock (HF), and sum-over-states methods. Time-dependent Hartree−Fock (TDHF) and coupled electron oscillator approaches have been used for the calculation of dynamic polarizabilities. Investigatons using the Pariser−Parr−Pople (PPP) Hamiltonian yielded scaling laws for polarizability of polyenes.[31,32] The saturation of the polarizability with increasing molecular size has been examined with PPP, semi empirical, and Hartree−Fock methods.[28,33−35] Density-functional calculations of the polarizabilities of conjugated oligomers using small basis sets do not compare well with known experimental values.[36] More accurate calculations of the polarizability of conjugated systems require larger basis sets as well as a suitable treatment of electron correlation.[37]

The above-mentioned applications of polarizability stem from the design of conjugated materials with specifically desired optical properties in the weak field regime. When molecules are placed in strong electromagnetic fields, such as the electric field of a laser, they not only undergo electronic excitation and internal conversion but also may ionize, which changes their optical properties considerably. To control and predict the outcomes of laser−matter interaction, knowledge of the optical properties of the various transient species involved in the excitation process is required. For example, recent measurements in strong-field laser chemistry of organic molecules[38−41] suggest that the formation of radical cations plays a major role in the laser−matter interaction. It is becoming increasingly clear that processes in the manifold of excited states of the ion are as important as those occurring in the neutral manifold before ionization. These processes are governed by the optical properties of the nascent species immersed in the laser field. Thus, to understand and predict the outcomes of strong-field laser−molecule interaction, one needs to know the radical cation polarizability, as well as that of the neutral molecules. Although optical properties of neutral organic molecules (gas-phase, liquid,

* To whom correspondence should be addressed. E-mail: hbs@chem.wayne.edu.
[†] Department of Chemistry, Wayne State University.
[‡] Department of Chemistry, Temple University.
[§] Center for Advanced Photonics Research, Temple University.
[||] Department of Physics, Temple University.
[⊥] Institute for Scientific Computing, Wayne State University.

10.1021/jp048864k CCC: $27.50 
Published on Web 11/19/2004

or solid) are routinely measured by spectrochemical methods, much less experimental information exists regarding of ionic species, due to difficulty of producing significant quantities of ions in gas phase.

Recently, a model of nonresonant strong field molecular laser excitation[38,39,42,43] was shown to agree quantitatively with experiment on a series of large organic molecules.[38,39] In this theory, a molecule subjected to a strong oscillating electric field undergoes a series of successive nonadiabatic energy absorption stages, resulting ionization, and fragmentation. At each stage of this sequential process, the rate-limiting step is the transfer of the electron population from the system's ground electronic state to the manifold of excited states via a Landau−Dykhne type doorway transition.[44] The transition probability depends sensitively on a key electronic property of a molecule, its polarizability, the calculation of which is the main subject of this paper.

The majority of molecular physics experiments are performed in the near-infrared ($\lambda \sim 800$ nm) wavelength region, where the energy of the laser photon, $\hbar\omega \sim 1.55$ eV, is smaller than the typical energy gap, $\Delta \sim 2-3$ eV, separating the ground electronic state from the excited-state manifold in a representative conjugated polyatomic molecule. In the weak-field regime (at laser intensities less than $10^{12}$ W·cm$^{-2}$), the nonresonant electronic response of an atom or molecule to this low-frequency laser field is adiabatic.[45] Under such adiabatic conditions, knowledge of field-free optical properties, e.g., static polarizabilities, is sufficient for a theoretical understanding of the interaction. However, in the majority of strong-field experiments involving polyatomic molecules, nonadiabatic processes of energy deposition are expected to occur. At sufficiently high laser intensities and/or frequencies where the coupling becomes highly nonadiabatic, laser fields induce a collective response of the electrons that results in irreversible energy deposition.[38,39,42,43] The probability of nonadiabatic electronic transitions depends sensitively on the frequency of the driving laser field. It is natural then, that frequency-dependent optical properties of molecules and their ions should be of great interest for predicting the probability of nonadiabatic processes.

Gas-phase polarizabilities for molecular ions (and dynamic polarizabilities in particular) are very difficult to obtain experimentally. However, the calculation of polarizabilities of ions is no more difficult than for neutrals. Static isotropic polarizabilities of molecular ions have been studied theoretically, although not as extensively as for neutral molecules. For example, the static polarizabilities of the molecular ions of naphthalene have been calculated[46,47] for charge states of the ion ranging from +2 to −2 and varies from 15 to 25 Å$^3$. However, it is dynamic polarizabilities (of both neutral molecules and their cations) that are primarily relevant in the investigations of laser−molecule interaction. To the best of our knowledge, dynamic polarizabilities have not received the attention they deserve, either theoretically or experimentally.

In this paper, we describe a theoretical study of the static and dynamic polarizabilities of two series of polyatomic molecules and their molecular ions. The trends in polarizability are investigated as a function of molecular size and $\pi$ electron conjugation. First, the level of theory is validated by comparing calculated results with experiment for a number of neutral molecules and with high level calculations on several of the smaller neutral molecules and their cations. Then we use the same level of theory to compute the static and dynamic polarizabilities of polyenes (from butadiene, $C_4H_6$, to octadecanonene, $C_{18}H_{20}$) and polyacenes (from benzene, $C_6H_6$, to tetracene, $C_{18}H_{12}$). To aid the understanding of the trends in these series, we have developed qualitative and semiquantitative relations between the sets of data on static and dynamic polarizabilities.

## Computational Method

Calculations were carried out with the development version of the GAUSSIAN[48] series of programs. Several levels of theory were used to compute polarizabilities: closed shell and restricted open shell Hartree−Fock (HF and ROHF), density functional theory (DFT) with the PBE0 hybrid functional[49,50] (also known as PBE1PBE), closed shell and restricted open shell second-order Moller−Plesset perturbation theory[51−55] (MP2 and ROMP2), and closed shell and spin unrestricted coupled cluster theory with singles and doubles excitations[56−59] (CCSD and UCCSD). The 6-31G(d) basis set[60,61] was used for HF, DFT, MP2, and CCSD calculations and is a split valence basis augmented with one set of polarization functions on the carbon atoms. The 6-311+G(2d,2p) basis set[62−65] was used for the HF and DFT calculations and is a triple split valence basis augmented with two sets of polarization functions on all atoms and one set of diffuse functions on carbon atoms. Geometries were optimized at the MP2/6-31G(d) and PBE0/6-311+G(2d,2p) levels of theory for the neutrals and cations of the linear polyenes and polyacenes.

Density functional methods using the local density approximation (LDA) have not been considered because they consistently overestimate the polarizability due to the locality of LDA.[76] DFT methods using the generalized gradient approximation (GGA) include the gradient of the density and involve a fit to selected experimental data and fulfillment of a number of basic physical constraints. Hybrid functionals mixes in a predefined amount of HF exchange with a GGA functional. Among the frequently used hybrid functionals, PBE0 gives remarkably good vertical excitation energies[72] and polarizabilities.[72,74] The recently developed Vignale−Kohn current-density-functional seems to give very promising results for long $\pi$ conjugated systems.[76,77] Although not available for the present study, it will be worthwhile to consider in future work.

The static first-order polarizability, $\alpha(0)$, and dynamic first-order polarizability, $\alpha(\omega)$, were calculated using an analytical derivative approach[66]

$$\alpha_{ij}(\omega) = -\frac{\partial^2 W}{\partial E_{\omega i}\partial E_{0j}} \tag{1}$$

where $W = \langle\psi|\hat{H} - i\partial/\partial t|\psi\rangle/\langle\psi|\psi\rangle$ is the pseudo energy, $E_{\omega i}$ is the frequency-dependent electric field in the $i$th direction, and $E_{0j}$ is the static electric field. The isotropic polarizability is given by the average of the diagonal elements of the polarizability tensor,

$$\alpha_{\mathrm{iso}} = \frac{1}{3}(\alpha_{xx} + \alpha_{yy} + \alpha_{zz}) \tag{2}$$

The sum-over-states approach yields the same value for both $\alpha(0)$ and $\alpha(\omega)$ as the energy derivative method but involves the rather difficult task of computing all the singly excited states and their transition dipole moments from the ground state. However, it is quite useful for analyzing the physical meaning of the trends in the polarizabilities. In this formalism, the tensor elements of the static and dynamic polarizability are given, respectively, by

$$\alpha_{ij}(0) = 2\sum_n \frac{\mu_i^{gn}\mu_j^{ng}}{\hbar\omega_{gn}} \quad (3)$$

$$\alpha_{ij}(\omega) = \sum_n \left( \frac{\mu_i^{gn}\mu_j^{ng}}{\hbar\omega_{gn} - \hbar\omega} + \frac{\mu_j^{gn}\mu_i^{ng}}{\hbar\omega_{gn} + \hbar\omega} \right) = 2\sum_n \left( \frac{\mu_i^{gn}\mu_j^{ng}}{\hbar\omega_{gn} - (\hbar\omega^2)/\omega_{gn}} \right) \quad (4)$$

where **e** is the unit vector in the electric field direction, so that $\mu_i^{gn} = \langle\psi_g^{(0)}|\sum e_a i_a |\psi_n^{(0)}\rangle$ is the transition dipole moment from the ground state to state *n* in the ***i***th direction, $\hbar\omega_{gn} = E_n - E_g$ is the transition energy, and $\hbar\omega$ is the photon energy.

The excited-state energies, $E_n$, were computed at the PBE0/6-311+G(2d,2p) level of theory using time-dependent density functional theory (TDDFT).[67−71] In the framework of the sum-over-states approach, these were used to determine whether the polarizabilities are dominated by nonresonant collective multielectron response or by resonant state-specific response. The excitation energies were also employed to reveal the scaling relations between the static and dynamic polarizabilities of the neutrals and cations.

## Results and Discussion

To establish an appropriate computational method for studying the dynamic polarizabilities of the polyene and polyacene neutrals and cations, we compared the HF, PBE0, MP2, and CCSD levels of theory for ethylene, butadiene, hexatriene, octatetraene, and their respective molecular +1 cations. The PBE0 functional was selected because it yields better static and dynamic polarizabilities and excitation energies for small molecules than B3LYP and other frequently used functionals.[72−74] As noted above, other new functionals may also give similar results. The 6-31G(d) basis set was chosen to make the CCSD polarizabilities computationally affordable for octatetraene. Table 1 lists the components of the calculated polarizability tensors, and Figure 1 shows the axial components of the polarizabilities. For the neutral systems, the polarizabilities obtained at the Hartree−Fock and PBE0 levels are very similar. The polarizabilities calculated at MP2 and CCSD levels agree well with each other and are lower than the HF and DFT results. This concurs very well with previous results for linear polyenes at the HF and MP2 levels with similar basis sets.[75−78] The PBE0 polarizability of octatetraene is 4% greater than the HF polarizability and 18−23% greater than the MP2 and CCSD polarizabilities. For the cations, the ROMP2 and UCCSD values also agree well with each other. In contrast to the neutrals, the ROHF and UPBE0 polarizabilities are very close to the MP2 and CCSD results. Overall, among the applied levels of theory, the polarizabilities vary by 9% for ethylene, 16% of butadiene, 4% for hexatriene, and 10% for octatetraene relative to the mean value. These results are quite encouraging, because much larger systems can be studied with HF and DFT approaches than with conventional correlated methods.

Table 2 compares the experimental values of static isotropic polarizabilities for a number of polyenes and polyacenes with our calculations at the HF/6-311+G(2d,2p) and PBE0/6-311+G(2d,2p) levels of theory. Previous calculations for various small molecules indicate that two sets of polarization functions and a set of diffuse functions are generally needed to obtain satisfactory agreement with experimental polarizabilities.[79] However, for the axial polarizability of larger polyenes, there is less need for large basis sets.[17] Butadiene is the only polyene for which experimental polarizability has been reported, and it has also been studied with a variety of theoretical methods and a wide range of basis sets.[78,80−84] The polarizabilities of butadiene calculated in the present work are 6.52, 8.10, and 8.13 Å$^3$ at the PBE0/6-31G(d), PBE0/6-311+G(2d,2p), and HF/6-311+G(2d,2p) levels of theory, respectively. The value of 8.10 Å$^3$ fortuitously agrees perfectly with the experimental value of 8.10 Å$^3$ obtained from an extrapolation of refractivity data to infinite wavelength.[78,85] These results confirm once more that to accurately calculate the polarizability of smaller polyenes, one needs larger basis set (cf. Hurst).[17]

Calculations for benzene, naphthalene, anthracene, and tetracene agree well with experimental results. Specifically, the calculated values differ from experimental ones by 0.3−10% at the HF/6-311+G(2d,2p) level of theory and 1.5−15% at the PBE0/6-311+G(2d,2p) level of theory. For a variety of small molecules, calculations with a more flexible basis set[79] (developed by Sadlej specifically for molecular properties such as polarizabilities) yield results that are closer to experiment.[72] However, this basis set is not practical for the larger members of either series.

When the same method is used for the ions, the calculated values are expected to be of similar quality and can be used with confidence in the absence of experimental data for these systems. Table 2 also shows calculated and experimental single excitation energies of three of the neutral linear polyenes and four of the polyacenes. For the lowest energy dipole-allowed

**TABLE 1: Static Polarizabilities of Neutral and +1 Cations of Ethylene, Butadiene, Hexatriene, and Octatetraene Calculated at the HF, PBEO, MP2, and CCSD Levels of Theory with the 6-31G(d) Basis Set[a]**

| molecule | level | $\alpha_{xx}$ | $\alpha_{yy}$ | $\alpha_{zz}$ | $\alpha_{iso}$ |
|---|---|---|---|---|---|
| ethylene | HF | 2.95 | 1.24 | 4.84 | 3.01 |
| | PBE0 | 2.99 | 1.27 | 4.57 | 2.94 |
| | MP2 | 2.97 | 1.21 | 4.29 | 2.83 |
| | CCSD | 2.95 | 1.21 | 4.31 | 2.82 |
| ethylene$^{+1}$ | ROHF | 2.45 | 1.14 | 4.83 | 2.81 |
| | UPBE0 | 2.46 | 1.19 | 3.92 | 2.52 |
| | ROMP2 | 2.45 | 1.14 | 3.71 | 2.43 |
| | UCCSD | 2.44 | 1.14 | 4.14 | 2.57 |
| butadiene | HF | 5.44 | 2.27 | 12.09 | 6.60 |
| | PBE0 | 5.63 | 2.32 | 11.61 | 6.52 |
| | MP2 | 5.54 | 2.22 | 10.34 | 6.03 |
| | CCSD | 5.48 | 2.22 | 10.26 | 5.98 |
| butadiene$^{+1}$ | ROHF | 2.78 | 2.15 | 12.91 | 5.95 |
| | UPBE0 | 5.28 | 2.20 | 12.36 | 6.61 |
| | ROMP2 | 1.53 | 2.13 | 13.95 | 5.24 |
| | UCCSD | 5.29 | 2.12 | 13.79 | 7.07 |
| hexatriene | HF | 7.88 | 3.28 | 23.04 | 11.40 |
| | PBE0 | 8.20 | 3.35 | 22.99 | 11.51 |
| | MP2 | 8.02 | 3.21 | 19.36 | 10.20 |
| | CCSD | 7.94 | 3.21 | 18.78 | 9.98 |
| hexatriene$^{+1}$ | ROHF | 8.37 | 3.15 | 29.04 | 13.52 |
| | UPBE0 | 7.88 | 3.21 | 27.32 | 12.80 |
| | ROMP2 | 8.64 | 3.09 | 28.02 | 13.24 |
| | UCCSD | 7.85 | 3.09 | 29.69 | 13.54 |
| octatetraene | HF | 10.31 | 4.29 | 37.74 | 17.44 |
| | PBE0 | 10.74 | 4.37 | 39.22 | 18.11 |
| | MP2 | 10.45 | 4.20 | 31.32 | 15.32 |
| | CCSD | 10.38 | 4.19 | 29.67 | 14.75 |
| octatetraene$^{+1}$ | ROHF | 12.58 | 4.14 | 49.95 | 22.22 |
| | UPBE0 | 10.47 | 4.22 | 49.44 | 21.38 |
| | ROMP2 | 4.09 | 3.05 | 50.11 | 19.08 |
| | UCCSD | 10.46 | 4.07 | 52.49 | 22.34 |

[a] Polarizabilties were calculated at the MP2/6−31(d) optimized geometries for both neutral molecules and molecular ions.

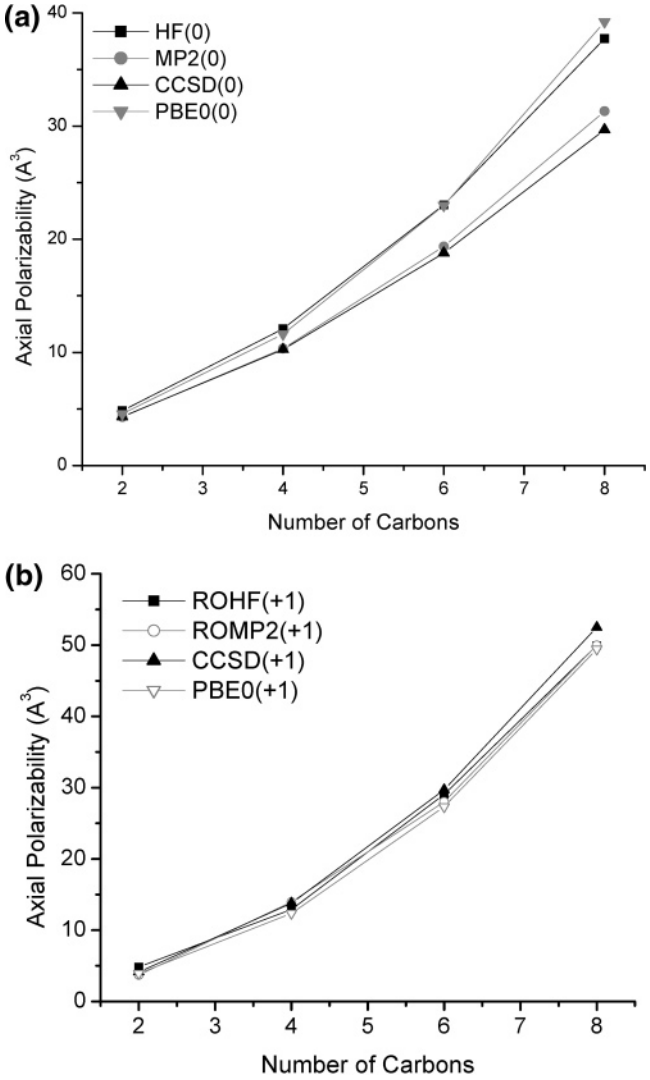


**Figure 1.** Static and dynamic axial polarizabilities of the linear polyenes and their cations as a function of carbon chain length, calculated using HF, PBE0, MP2, and CCSD with the /6-31G(d) basis set.

transitions, the differences range from 0.02 to 0.3 eV (1−8%), which is typical for the PBE0/6-311+G(2d,2p) level of theory.[73]

The results shown in Tables 1 and 2 serve to validate the computational methodology, which is used to calculate the polarizabilities for the neutrals and singly charged cations of polyenes and polyacenes. Tables 3 and 4 list the principal components of the polarizability tensors, as well as the isotropic polarizabilities. There is good agreement between the HF and PBE0 calculations. As was found previously for other functionals,[36] the differences increase with system size, rising to 21% for $C_{18}H_{20}$. Notably, the polarizabilities of the cations are generally larger than that of the corresponding neutrals, and this difference increases with the size of the system. Tables 3 and 4 also present the dynamic polarizabilities calculated at 800 nm (equal to 1234.7 cm$^{-1}$ or 1.55 eV). As expected, the near-IR $\alpha(\omega)$ are larger than the $\alpha(0)$ but, unexpectedly, the effect is much greater for the cations than for the neutrals. The static and frequency-dependent $\alpha_{iso}$ for the linear polyenes series and the polycyclic aromatics series are plotted in Figures 2 and 3, respectively. In all cases, the polarizabilities show a supralinear increase with system size. In the next subsections, we will examine these trends more closely.

**Size Dependence of the Polarizabilities.** It is well-known that for a homologous series of nonconjugated molecules in the same charge state, polarizabilities generally increase linearly with increasing number of charged particles. However, for conjugated systems composed of strongly interacting subunits, such as the polyenes and polyacenes considered in the present work, model calculations have shown that $\alpha$ increases supralinearly for small oligomers.[16−19,26,32,86−89] Eventually, the rate of increase per subunit saturates,[19,21,25,26,86,88,90] but this occurs for systems significantly larger than those in the current study. The $\alpha_{iso}$ of the polyenes, polyacenes, and their cations are plotted in Figures 2 and 3 as a function of system size. Both series clearly show the expected supralinear increase with size. A closer look at the polarizability tensor reveals that this nonlinearity is almost exclusively due to the component along the long molecular axis, as expected. By contrast, the two components perpendicular to the long axis increase approximately linearly with the increasing chain length, i.e., proportionally to the number of charged particles. This linear increase in the two components perpendicular to the long axis is also observed for polythiophenes.[26] For both series, the $\alpha$ along the long axis rises much faster than linearly as a result of increasing $\pi$ electron conjugation as the molecule becomes longer. In this case, in accordance with a simple coupled oscillator picture,[91] the energy difference between the ground state and the first excited state decreases with increasing chain length. Furthermore, the transition dipole matrix elements increase with the system size. Both effects can be seen in Tables 5 and 6, which list the energies and transition dipoles for the lowest excited states with large contributions to the axial polarizabilities. Thus, in the sum-over-states picture, eqs 3 and 4, the denominators become smaller and the numerators become larger, thereby increasing the $\alpha$ more rapidly than linearly with increasing chain length.

These results contribute to the ongoing discussion of influence of electronic system's anisotropy on the mechanisms of its coupling with linearly polarized laser fields.[92,93] The supralinear increase in the longitudinal component of the polarizability with increasing molecular size should significantly affect the orientational selectivity of the coupling of these molecules with the laser field. Indeed, an increasing anisotropy of an electronic system's response is expected to result in more efficient coupling with the laser of the subset of molecules aligned with the direction of polarization of the electric field. This premise is implicit in models of molecular interaction with strong laser fields, e.g., the structure-based field ionization model,[94,95] the

**TABLE 2: Calculated and Experimental Static Isotropic Polarizabilities and Excited-State Energies for Selected Neutral Molecules**

| | | polarizability (Å$^3$) | | excited-state energy (eV) | |
|---|---|---|---|---|---|
| molecule | level | $\alpha_{calc}$[a] | $\alpha_{exp}$ | $S_{1calc}$[a] | $S_{1exp}$ |
| | | Linear Polyenes | | | |
| butadiene | PBE0 | 8.10 | 8.10[74,75] | 5.75 | 5.73[88] |
| | HF | 8.13 | | | |
| hexatriene | PBE0 | 13.77 | | 4.75 | 4.93[88] |
| | HF | 13.59 | | | |
| octatetraene | PBE0 | 21.07 | | 4.09 | 4.41[89] |
| | HF | 20.32 | | | |
| | | Polyacenes | | | |
| benzene | PBE0 | 9.89 | 10.38[b] | | |
| | HF | 9.77 | | | |
| naphthalene | PBE0 | 17.29 | 17.03[b] | 4.37 | 4.45 |
| | HF | 16.88 | | | |
| anthracene | PBE0 | 26.33 | 25.55[b] | 3.29 | 3.84[90] |
| | HF | 25.47 | | | 3.45[91] |
| tetracene | PBE0 | 37.02 | 32.27[b] | 2.50 | 2.60[92] |
| | HF | 35.53 | | | 2.72[93] |

[a] Calculated at the PBE0/6-311+G(2d,2p) geometries. [b] Average of experimental values quoted in ref 94.

**TABLE 3: Static and Dynamic Polarizabilities[a] (Å$^3$) of Neutral Polyenes and Polyacenes Calculated at the PBE0/6-311+G(2d,2p) and HF/6-311+G(2d,2p) Levels of Theory[b]**

| | | $\omega = 0$ cm$^{-1}$ | | | | $\omega = 1234.7$ cm$^{-1}$ | | | |
|---|---|---|---|---|---|---|---|---|---|
| molecule | level | $\alpha_{xx}$ | $\alpha_{yy}$ | $\alpha_{zz}$ | $\alpha_{iso}$ | $\alpha_{xx}$ | $\alpha_{yy}$ | $\alpha_{zz}$ | $\alpha_{iso}$ |
| | | | | Linear Polyenes | | | | | |
| butadiene | PBE0 | 6.34 | 5.12 | 12.82 | 8.10 | 6.41 | 5.21 | 13.39 | 8.34 |
| | HF | 6.02 | 5.23 | 13.12 | 8.13 | | | | |
| hexatriene | PBE0 | 9.21 | 7.11 | 24.98 | 13.77 | 8.32 | 7.22 | 26.90 | 14.14 |
| | HF | 8.73 | 7.26 | 24.78 | 13.59 | | | | |
| octatetraene | PBE0 | 12.30 | 9.06 | 41.85 | 21.07 | 12.48 | 9.19 | 46.75 | 22.81 |
| | HF | 11.40 | 9.26 | 40.29 | 20.32 | | | | |
| decapentene | PBE0 | 15.16 | 11.01 | 64.19 | 30.12 | 15.40 | 11.16 | 74.82 | 33.79 |
| | HF | 14.09 | 11.33 | 60.51 | 28.64 | | | | |
| dodecahexene | PBE0 | 18.00 | 12.95 | 92.07 | 41.01 | 18.30 | 13.12 | 112.57 | 48.00 |
| | HF | 16.69 | 13.24 | 82.21 | 37.38 | | | | |
| tetradecaheptene | PBE0 | 20.85 | 14.88 | 125.55 | 53.76 | 21.22 | 15.03 | 161.78 | 66.03 |
| | HF | 19.32 | 15.22 | 108.11 | 47.55 | | | | |
| hexadecaoctene | PBE0 | 23.68 | 16.82 | 164.77 | 68.42 | 24.14 | 17.03 | 224.99 | 88.72 |
| | HF | 21.95 | 17.20 | 137.03 | 58.73 | | | | |
| octadecanonene | PBE0 | 26.53 | 18.75 | 209.10 | 84.79 | 27.08 | 18.99 | 303.68 | 116.58 |
| | HF | 24.57 | 19.18 | 167.12 | 70.29 | | | | |
| | | | | Polyacenes | | | | | |
| benzene | PBE0 | 11.67 | 6.32 | 11.67 | 9.89 | 11.94 | 6.40 | 11.94 | 10.09 |
| | HF | 11.41 | 6.49 | 11.41 | 9.77 | | | | |
| naphthalene | PBE0 | 17.86 | 9.34 | 24.67 | 17.29 | 18.33 | 9.45 | 25.63 | 17.80 |
| | HF | 17.31 | 9.59 | 23.73 | 16.88 | | | | |
| anthracene | PBE0 | 24.15 | 12.31 | 42.54 | 26.33 | 25.05 | 12.45 | 44.97 | 27.49 |
| | HF | 23.61 | 12.63 | 40.17 | 25.47 | | | | |
| tetracene | PBE0 | 30.66 | 15.26 | 65.13 | 37.02 | 32.68 | 15.44 | 70.17 | 39.43 |
| | HF | 30.50 | 15.66 | 60.44 | 35.53 | | | | |

[a] $\alpha_{xx}$ is the polarizability along the short axis in the plane of the molecule, $\alpha_{yy}$ is the polarizability perpendicular to the plane, $\alpha_{zz}$ is the polarizability along the long molecular axis, and $\alpha_{iso}$ is the isotropic polarizability. [b] Polarizabilities were calculated at the PBE0/6-311+G(2d, 2p) geometries.

**TABLE 4: Static and Dynamic Polarizabilities[a] (Å) of Polyene and Polyacene Cations Calculated at the PBE0/6-311+G(2d,2p) and HF/6-311+G(2d,2p) Levels of Theory[b]**

| | | $\omega = 0$ cm$^{-1}$ | | | | $\omega = 1234.7$ cm$^{-1}$ | | | |
|---|---|---|---|---|---|---|---|---|---|
| molecular ion | level | $\alpha_{xx}$ | $\alpha_{yy}$ | $\alpha_{zz}$ | $\alpha_{iso}$ | $\alpha_{xx}$ | $\alpha_{yy}$ | $\alpha_{zz}$ | $\alpha_{iso}$ |
| | | | | Linear Polyenes | | | | | |
| butadiene$^{+1}$ | UPBE0 | 5.62 | 3.78 | 12.99 | 7.46 | 7.14 | 4.01 | 12.87 | 8.01 |
| | ROHF | 3.70 | 3.94 | 13.17 | 6.93 | | | | |
| hexatriene$^{+1}$ | UPBE0 | 8.44 | 5.69 | 28.58 | 14.24 | 8.68 | 5.75 | 32.78 | 15.74 |
| | ROHF | 8.79 | 5.94 | 30.19 | 14.98 | | | | |
| octatetraene$^{+1}$ | UPBE0 | 11.29 | 7.61 | 52.16 | 23.69 | 11.77 | 7.69 | 64.30 | 27.92 |
| | ROHF | 13.21 | 7.93 | 52.98 | 24.71 | | | | |
| decapentene$^{+1}$ | UPBE0 | 14.13 | 9.54 | 84.93 | 36.20 | 15.37 | 9.64 | 114.70 | 46.57 |
| | ROHF | 15.46 | 9.92 | 84.33 | 36.57 | | | | |
| dodecahexene$^{+1}$ | UPBE0 | 16.99 | 11.47 | 128.11 | 52.19 | 44.01 | 11.59 | 238.35 | 97.98 |
| | ROHF | 19.49 | 11.92 | 124.36 | 51.92 | | | | |
| tetradecaheptene$^{+1}$ | UPBE0 | 19.86 | 13.40 | 183.05 | 72.11 | 17.70 | 13.54 | 301.89 | 111.04 |
| | ROHF | 22.65 | 13.91 | 174.18 | 70.25 | | | | |
| hexadecaoctene$^{+1}$ | UPBE0 | 22.74 | 15.33 | 251.12 | 96.40 | 21.50 | 15.50 | 492.80 | 176.60 |
| | ROHF | 26.73 | 15.91 | 234.16 | 92.26 | | | | |
| octadecanonene$^{+1}$ | UPBE0 | 25.64 | 17.27 | 333.68 | 125.53 | 24.71 | 17.45 | 818.45 | 286.87 |
| | ROHF | 30.46 | 17.90 | 305.11 | 117.82 | | | | |
| | | | | Polyacenes | | | | | |
| benzene$^{+1}$ | UPBE0 | 10.08 | 5.00 | 11.21 | 8.76 | 10.31 | 5.05 | 11.70 | 9.02 |
| | ROHF | 9.68 | 5.17 | 12.33 | 9.06 | | | | |
| naphthalene$^{+1}$ | UPBE0 | 17.31 | 7.98 | 26.45 | 17.24 | 18.00 | 8.06 | 31.58 | 19.21 |
| | ROHF | 17.25 | 8.28 | 33.59 | 19.71 | | | | |
| anthracene$^{+1}$ | UPBE0 | 23.38 | 10.94 | 49.25 | 27.85 | 24.61 | 11.04 | 65.63 | 33.76 |
| | ROHF | 22.85 | 11.29 | 50.67 | 28.27 | | | | |
| tetracene$^{+1}$ | UPBE0 | 29.70 | 13.88 | 80.90 | 41.49 | 36.22 | 14.00 | 147.15 | 65.79 |
| | ROHF | 30.52 | 14.34 | 82.07 | 42.31 | | | | |

[a] $\alpha_{xx}$ is the polarizability along the short axis in the plane of the molecule, $\alpha_{yy}$ is the polarizability perpendicular to the plane, $\alpha_{zz}$ is the polarizability along the long molecular axis, and $\alpha_{iso}$ is the isotropic polarizability. [b] Polarizabilities were calculated at the PBE0/6-311+G(2d, 2p) geometries.

nonadiabatic multielectron excitation model,[38,39,42,43] and the nonadiabatic charge localization model.[96] Though the predictions of these models are well supported by experimental data, some other data on the strong-field ionization of polyatomic molecules (including some molecules used in this work) has been interpreted by Hankin et al.[92,93] as evidence for isotropic ionization yield from molecules of varying shapes. These quantitative results on the spatial dependence of the polarizability of conjugated $\pi$-electron systems suggest that the controversy is due to other factors, such as dark states or widely

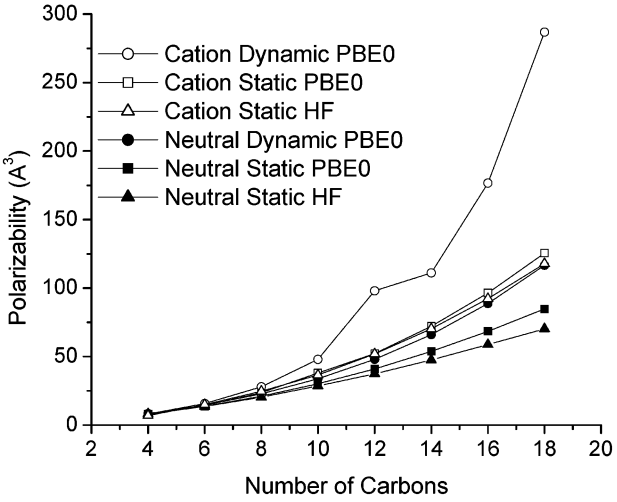


**Figure 2.** Static and dynamic isotropic polarizabilities of the linear polyenes and their cations as a function of carbon chain length, calculated using PBE0/6-311+G(2d,2p).

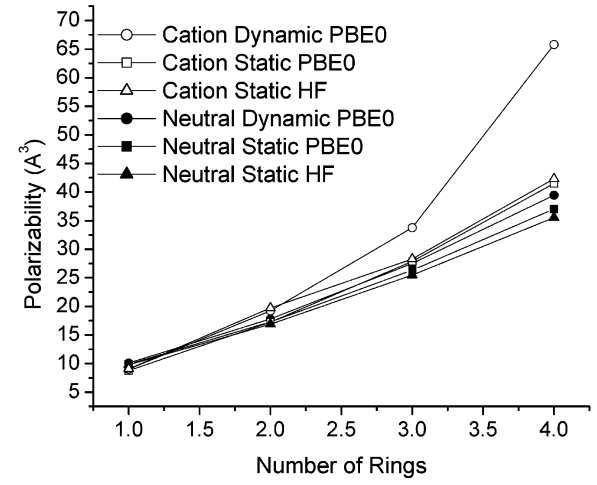


**Figure 3.** Static and dynamic isotropic polarizabilities of the polyacenes and their cations as a function of carbon chain length, calculated using PBE0/6-311+G(2d,2p).

varying chemical functionality. Thus, the present work is of current interest to the strong-field laser chemistry community.

**Charge-State Dependence of the Polarizabilities.** When a molecule is ionized, one of the electrons contributing to the polarizability is removed. Therefore, one might expect the polarizability of the cation to be smaller than that of the corresponding neutral. This is indeed the case for atoms and small molecules. For neutral Ne, the experimental polarizability is 0.392 $A^3$, whereas for the cation it is 0.192 $Å^3$.[97] Similar behavior is found in the case of butadiene (8.10 $Å^3$ calculated for the neutral and 7.46 $Å^3$ for the cation) and benzene (9.89 and 8.76 $Å^3$, respectively). However, for larger molecules, such as the extended conjugated systems examined in this study, the situation is more complicated. As can be seen from the data in Tables 3 and 4, the components of the polarizability perpendicular to the long molecular axis generally decrease upon ionization, showing behavior typical of small and weakly coupled systems. However, polarizabilities along the long axis of these molecules increase upon ionization for all members of the two series of molecules (except for benzene at the PBE0/6-311+G(2d,2p) level). Other than for butadiene and benzene, this increase more than offsets for the loss of polarizability in the other two directions.

As the sum-over-states analysis shows, for the polyenes, the increase in axial polarizability on ionization is primarily due to a decrease in the excitation energies appearing in the denominator of the sum-over-states formulas. Table 5 shows that lowest excitation energies are dominated by transitions from the highest occupied molecular orbital (HOMO) to the lowest unoccupied molecular orbital (LUMO); they decrease by 15−25% on ionization. The transition dipole matrix elements that appear in the numerator of the sum-over-states formulas remain nearly constant on ionization. For the polyacenes, the situation is more complicated, as indicated in Table 6. In the neutral systems, the configurations arising from the HOMO to LUMO+1 excitation and the HOMO−1 to LUMO excitation are nearly equal in energy. However, these configurations interact strongly forming symmetric and antisymmetric combinations and lift the near degerneracy.[98] The symmetric combination is lower in energy, but it has only a very small dipole matrix element in the longitudinal direction and therefore does not contribute much in the corresponding polarizability. The higher energy, antisymmetric combination has a larger transition dipole and by this virtue accounts for a substantial fraction of the axial polarizability. In the cation, the energies of the HOMO to LUMO+1 transition and the HOMO−1 to LUMO are appreciably different. As a result the linear combination of the two excited states that corresponds to the higher energy state has a larger coefficient for the HOMO to LUMO+1 transition and a slightly smaller transition dipole moment along the molecular axis, compared to the neutral. The lower energy state has a larger coefficient for the HOMO−1 to LUMO transition. This latter state has also a larger transition dipole along the molecular axis than the corresponding state in the neutral. Thus, it is the lower energy state that accounts for a significant fraction of the increase in the polarizability for the cation.

For short polyene neutrals and cations, the longitudinal component of the polarizability ($\alpha_{zz}$), can be modeled quite well by $\alpha_{zz} = aN^b$, where $N$ is the number of carbons.[15] The values of $b$ calculated for the neutral linear polyenes in Table 1 are 1.47. 1.54, 1.43, and 1.39 for the HF, PBE0, MP2, and CCSD levels of theory with the 6-31G(d) basis set. For the polyene cations in Table 1, $b = 1.86$. 1.82, 1.63, and 1.83 for the ROHF, UPBE0, ROMP2, and UCCSD levels of theory, respectively. Using the data in Table 3, $b = 1.71$ and 1.91 for the neutral polyene polarizabilities computed at the HF/6-311+G(2d,2p) and PBE0/6-311+G(2d,2p) levels of theory. The values of $b$ calculated for the polyene cations in Table 4, 2.08 by ROHF, and 2.21 by UPBE0, are 16−22% higher than for the neutrals. All of these calculations indicate that experimental polarizabilities should also show a larger scaling factor for the cations than for the neutrals.

**Frequency Dependence of the Polarizabilities.** For both series of molecules, the near-IR $\alpha(\omega)$ are larger than the $\alpha(0)$ by as much as a factor of 2.3. Again, this can be readily understood when both $\alpha(\omega)$ and $\alpha(0)$ are expressed using the sum-over-states picture. The transition dipoles appearing in the numerators of both equations are the same, because the summation occurs over the same states. However, for each state, the contribution in eq 4 is smaller than in eq 3 because the excitation energies appearing in the denominator are reduced by the photon energy $\hbar\omega$. The increase is far more dramatic for the corresponding cations. Because the excitation energies for the polyene cations are smaller than for the neutrals, the reduction in the denominator of eq 4 due to the photon energy is proportionately greater. For the polyacenes, the lower energy state of the cation has a much larger transition dipole than the

**TABLE 5: Excited-State Energies and Transition Dipole Moments of Neutral and +1 Cations of Linear Polyenes Calculated Using TDDFT at the PBE0/6-311+G(2d,2p) Level of Theory**

| molecule | excited-state energy (eV) | electron transitions (TDDFT coefficients) | transition electric dipole moment components | | | oscillator strength |
|---|---|---|---|---|---|---|
| | | | *X* | *Y* | *Z* | |
| butadiene | 5.7453 | HOMO → LUMO (0.61) | −0.4851 | 0.0000 | 2.1024 | 0.4851 |
| butadiene+1 | 4.7828 | HOMO → LUMO (0.80)<br>HOMO−1 → LUMO+1 (0.17) | −0.4832 | 0.0000 | 1.9114 | 0.4832 |
| hexatriene | 4.7484 | HOMO → LUMO (0.60) | −1.0706 | 0.0000 | 2.8495 | 1.0779 |
| hexatriene+1 | 3.8849 | HOMO → LUMO (0.73)<br>HOMO−1 → LUMO+1 (−0.13) | −0.1157 | 0.0000 | 3.0482 | 0.8856 |
| octatetraene | 4.0878 | HOMO → LUMO (0.60) | −1.6054 | 0.0000 | 3.5280 | 1.5047 |
| octatetraene+1 | 3.3047 | HOMO → LUMO (0.70)<br>HOMO−1 → LUMO+1 (−0.14) | −1.8459 | 0.0000 | 3.5824 | 1.3149 |
| decapentene | 3.3248 | HOMO → LUMO (0.57) | −0.3397 | 0.0000 | 4.9389 | 1.9963 |
| decapentene+1 | 2.8898 | HOMO → LUMO (0.66)<br>HOMO−1 → LUMO+1 (−0.15) | −0.1270 | 0.0000 | 4.9727 | 1.7519 |
| dodecahexene | 3.2629 | HOMO → LUMO (0.60) | −0.3247 | 0.0000 | 5.4099 | 2.3480 |
| dodecahexene+1 | 2.5728 | HOMO → LUMO (0.64)<br>HOMO−1 → LUMO+1 (−0.17) | −0.1320 | 0.0000 | 5.8876 | 2.1860 |
| tetradecaheptene | 2.9864 | HOMO → LUMO (0.60) | −0.3297 | 0.0000 | 6.1337 | 2.7606 |
| tetradecaheptene+1 | 2.3209 | HOMO → LUMO (0.62)<br>HOMO−1 → LUMO+1 (−0.18) | −0.1312 | 0.0000 | 6.7790 | 2.6140 |
| hexadecaoctene | 2.7632 | HOMO → LUMO (0.60) | −0.3362 | 0.0000 | 6.8299 | 3.1655 |
| hexadecaoctene+1 | 2.1146 | HOMO → LUMO (0.60)<br>HOMO−1 → LUMO+1 (−0.20) | −0.1112 | 0.0000 | 7.6542 | 3.0357 |
| octadecanonene | 2.5815 | HOMO → LUMO (0.60) | −0.3439 | 0.0000 | 7.4967 | 3.5619 |
| octadecanonene+1 | 1.9418 | HOMO → LUMO (0.54)<br>HOMO−1 → LUMO+1 (−0.21)<br>HOMO−2 → LUMO+2 (0.11) | −0.1291 | 0.0000 | 8.5151 | 3.4501 |

**TABLE 6: Excited-State Energies and Transition Dipole Moments of Neutral and +1 Cations of Linear Polyacenes Calculated Using TDDFT at the PBE0/6-311+G(2d,2p) Level of Theory**

| molecule | excited-state energy (eV) | electron transitions (TDDFT coefficients) | transition electric dipole moment components | | | oscillator strength |
|---|---|---|---|---|---|---|
| | | | *X* | *Y* | *Z* | |
| benzene | 5.5157 | HOMO−1 → LUMO (−0.49)<br>HOMO−1 → LUMO +1 (0.15)<br>HOMO → LUMO (0.15)<br>HOMO → LUMO +1 (0.49) | −0.0001 | 0.0000 | −0.0005 | 0.0000 |
| | 7.0785 | HOMO−1 → LUMO (−0.24)<br>HOMO−1 → LUMO +1 (0.34)<br>HOMO → LUMO (−0.34)<br>HOMO → LUMO +1 (−0.24) | 0.5963 | 0.0000 | 1.7714 | 0.6058 |
| benzene +1 | 4.6085 | HOMO → LUMO (0.92)<br>HOMO−1 → LUMO +1 (0.09) | 0.0045 | 0.0000 | −0.4592 | 0.0274 |
| | 7.1045 | HOMO → LUMO (0.27)<br>HOMO−1 → LUMO +1 (0.67) | 0.0061 | 0.0000 | 1.4856 | 0.3841 |
| naphthalene | 4.5523 | HOMO−1 → LUMO (0.51)<br>HOMO → LUMO +1 (0.52) | 0.0000 | 0.0000 | −0.0144 | 0.0000 |
| | 5.9742 | HOMO−1 → LUMO (0.43)<br>HOMO → LUMO +1 (−0.42) | 0.0000 | 0.0000 | 2.9633 | 1.2852 |
| naphthalene +1 | 2.0052 | HOMO−1 → LUMO (0.98)<br>HOMO → LUMO +1 (0.12) | 0.0000 | 0.0000 | 1.0958 | 0.0590 |
| | 5.9867 | HOMO−1 → LUMO (0.57)<br>HOMO → LUMO +1 (−0.34) | 0.0000 | 0.0000 | 2.6420 | 1.0238 |
| anthracene | 3.9469 | HOMO−1 → LUMO (0.50)<br>HOMO → LUMO +1 (0.51) | 0.0000 | 0.0000 | −0.0385 | 0.0001 |
| | 5.2529 | HOMO−1 → LUMO (0.43)<br>HOMO → LUMO +1 (−0.42) | 0.0000 | 0.0000 | 3.9833 | 2.0419 |
| anthracene +1 | 5.1736 | HOMO−1 → LUMO (0.99)<br>HOMO → LUMO +1 (0.11) | 0.0000 | 0.0000 | 3.6192 | 1.6603 |
| | 5.1736 | HOMO−1 → LUMO (0.58)<br>HOMO → LUMO +1 (−0.33) | 0.0000 | 0.0000 | 3.6192 | 1.6603 |
| tetracene | 3.5544 | HOMO−1 → LUMO (0.52)<br>HOMO → LUMO +1 (0.50) | 0.0000 | 0.0000 | −0.1202 | 0.0013 |
| | 4.7333 | HOMO−1 → LUMO (0.43)<br>HOMO → LUMO +1 (−0.41) | 0.0000 | 0.0000 | 4.8989 | 2.7830 |
| tetracene +1 | 1.6624 | HOMO−1 → LUMO (0.97)<br>HOMO → LUMO +1 (0.13) | 0.0000 | 0.0000 | −2.1314 | 0.1850 |
| | 4.6861 | HOMO−1 → LUMO (0.58)<br>HOMO → LUMO +1 (−0.32) | 0.0000 | 0.0000 | 4.4360 | 2.2592 |

neutral. This change in the numerator of eq 4 results in a larger difference between the static and dynamic polarizability for the cation than for the neutral.

The $\alpha(\omega)$ of dodecahexene cation is noticeably larger than that expected from the trends shown in Figure 2. The cause of this irregularity is that the frequency of the applied field, 800 nm (1.55 eV), is nearly resonant with the first excited state of the dodecahexene cation, 1.5352 eV (calculated by TDDFT with PBE0/6-311+G(2d,2p)). Figure 4 shows the response of the polarizability for dodecahexene, $C_{12}H_{14}$, as the frequency of the

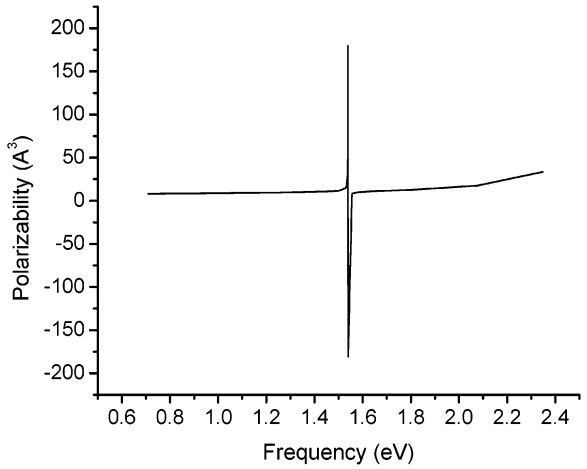


**Figure 4.** Isotropic polarizability of the ground state of positively charged ion of dodecahexene, $C_{12}H_{14}^{+}$, calculated in the range of laser frequencies including the resonance with the first excited state.

field is varied, revealing a discontinuity at the resonance energy, thus yielding an enhanced polarizability for the near-resonant case. This is an example of polarizability significantly affected by a resonance, i.e., state-specific response, in contrast to polarizability arising from the collective response of the electron density to the external field. For all other molecules and ions examined in this work, the collective response of the electrons is the dominant mechanism affecting polarizability.

The dramatic increase, rather than decrease in the polarizability along the longest direction upon ionization should have significant implications for the coupling of the cations with the laser field. The large polarizability of the ground electronic state results in a large dynamic Stark shift in the applied electric field. As shown in our other publications,[38,39] the large Stark shift of the ground electronic state should exponentially increase the probability of nonadiabatic electronic transitions to the excited-state manifold. Thus, when a system becomes more polarizable upon ionization, the probability of its further nonadiabatic excitation will exponentially increase. Conversely, when a cation is less polarizable than the corresponding neutral (which is typically the case for atoms and small molecules), the probability of nonadiabatic excitation of the cation will be exponentially reduced. For some polyatomic molecules, such as butadiene and benzene, this reduction in polarizability upon ionization results, in accordance with observations,[99,100] in increased probability of detecting intact molecular ions following nonresonant excitation. The search for a universal ionization method producing intact molecular ions has been a long-standing problem in molecular laser physics. Understanding of the evolution of a system's polarizability during the coupling with a laser pulse will allow for more accurate predictions of the intact molecular ion yield following strong-field excitation.

**Models for Predicting the Polarizabilities of the Cations.** In the discussion so far, we have described qualitatively some of the competing factors that play an important role in determining the polarizability as a function of the size, shape, and charge state of a molecule. The systematic changes in the excitation spectra suggest that the changes in the polarizability of neutral polyenes and their cations may be predicted semi-quantitatively. Except for state-specific cases, such as the α-(800 nm) of dodecahexene described above, many states contribute to the polarizability when computed using the sum-over-states formalism. In nonresonant cases, systematic changes in the entire spectrum of excited states have a greater effect on the calculated polarizability than specific changes in an individual state. Hence, there may exist simple scaling relations that take into account the changes in energy denominators of eq 3 and 4. The scaling factor can be estimated from the lowest energy excitation making significant contributions to the polarizability in the sum-over-states formalism. For example, the static polarizabilities of ions may be estimated from the static polarizabilities of the neutral by eq 5. The dynamic polarizabilities of ions may be estimated from the static polarizabilities of ions by eq 6 or using the dynamic polarizabilities of neutrals by eq 7:

$$\alpha(0)_{\text{cation}} = \alpha(0)_{\text{neutral}} \frac{\hbar\omega_{gs}^{0}}{\hbar\omega_{gs}^{+1}} \tag{5}$$

$$\alpha(\omega)_{\text{cation}} = \alpha(0)_{\text{cation}} \frac{\hbar\omega_{gs}^{+1}}{\hbar\omega_{gs}^{+1} - (\hbar\omega^2)/\omega_{gs}^{+1}} \tag{6}$$

$$\alpha(\omega)_{\text{cation}} = \alpha(\omega)_{\text{neutral}} \frac{\hbar\omega_{gs}^{0} - (\hbar\omega^2)/\omega_{gs}^{0}}{\hbar\omega_{gs}^{+1} - (\hbar\omega^2)/\omega_{gs}^{+1}} \tag{7}$$

where $\hbar\omega_{gs}^{0} = E_s^0 - E_g^0$ and $\hbar\omega_{gs}^{+1} = E_s^{+1} - E_g^{+1}$ refer to relevant excitation energies for the neutral and cation, respectively. Equation 6 is obtained from the ratio of eqs 3 and 4.

Some discretion is needed in selecting the excited states for eqs 5−7. Most importantly, the excited states chosen for both the neutral molecule and the corresponding cation must be dominated by the same orbital transitions. Table 5 shows that the lowest excited state for a neutral polyene and the corresponding state for the cation are both dominated by a HOMO to LUMO transition and have transition dipoles oriented along the long axis. Figure 5a shows that the simple scaling relations given by eqs 5−7 work remarkably well. On the other hand, the lowest excited states of polyacene involve a strong interaction between two transitions, and the weighting changes when the molecule is ionized. In this case, a simple scaling procedure does not work.

Even though eqs 5−7 give quite good results, excited-state calculations are costly for the larger molecules. Alternatively, it may be possible to estimate the scaling factor more cheaply using the orbital energies. Because the excitation energies for the polyenes are dominated by the HOMO to LUMO transitions, the trends in the excitation energies employed in eqs 5−7 can be approximated by using the HOMO−LUMO orbital energy differences:

$$\alpha(0)_{\text{cation}} = \alpha(0)_{\text{neutral}} \frac{\epsilon_{\text{LUMO}}^{0} - \epsilon_{\text{HOMO}}^{0}}{\epsilon_{\text{LUMO}}^{+1} - \epsilon_{\text{HOMO}}^{+1}} \tag{8}$$

$$\alpha(\omega)_{\text{cation}} = \alpha(0)_{\text{cation}} \frac{\epsilon_{\text{LUMO}}^{+1} - \epsilon_{\text{HOMO}}^{+1}}{(\epsilon_{\text{LUMO}}^{+1} - \epsilon_{\text{HOMO}}^{+1}) - (\hbar\omega)^2/(\epsilon_{\text{LUMO}}^{+1} - \epsilon_{\text{HOMO}}^{+1})} \tag{9}$$

$$\alpha(\omega)_{\text{cation}} = \alpha(\omega)_{\text{neutral}} \frac{(\epsilon_{\text{LUMO}}^{0} - \epsilon_{\text{HOMO}}^{0}) - (\hbar\omega)^2/(\epsilon_{\text{LUMO}}^{0} - \epsilon_{\text{HOMO}}^{0})}{(\epsilon_{\text{LUMO}}^{+1} - \epsilon_{\text{HOMO}}^{+1}) - (\hbar\omega)^2/(\epsilon_{\text{LUMO}}^{+1} - \epsilon_{\text{HOMO}}^{+1})} \tag{10}$$

where $\epsilon^0$ and $\epsilon^{+1}$ are the α orbital energies of the neutral and the cation, respectively. Figure 5b shows that the static and

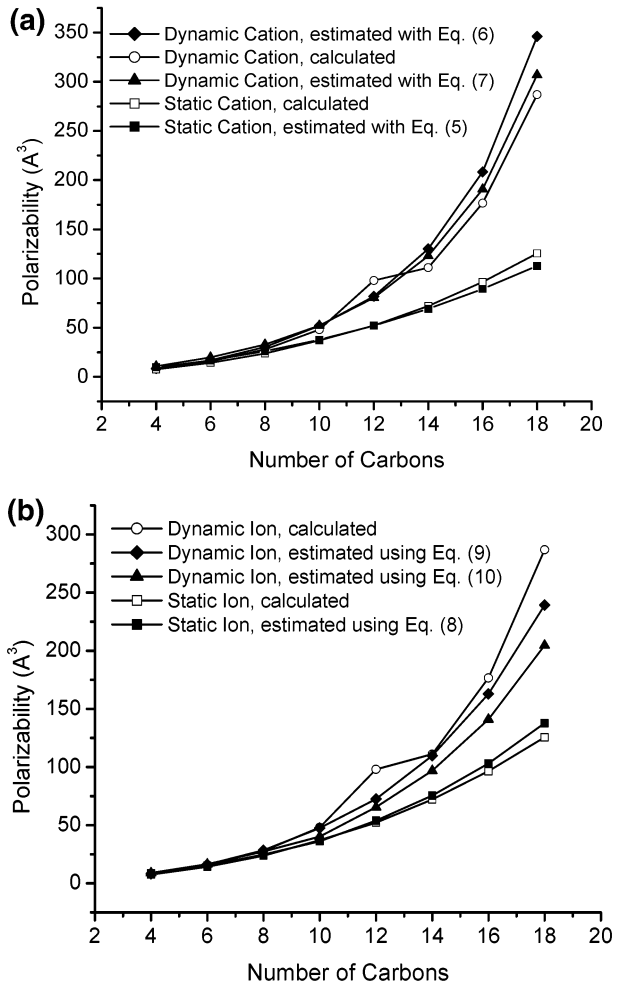


**Figure 5.** Static and dynamic isotropic polarizabilities of the cations of linear polyenes as a function of carbon chain length, calculated using PBE0/6-311+G(2d,2p) and using eqs 5−10.

dynamic polarizabilities of the polyene cations are approximated reasonably well by eqs 8−10, though not as well as by eqs 5−7.

## Conclusions

We have used Hartee-Fock and hybrid density functional calculations to investigate the static polarizabilities and the dynamic polarizabilities at $\lambda = 800$ nm of two sets polyatomic neutral molecules and their singly charged molecular cations. The first set is a series of eight all-trans linear polyenes; the second set consists of four polycyclic aromatics. The Hartree−Fock and PBE0 density-functional theory calculations are calibrated by comparing the results with those obtained by second-order Moller−Plesset perturbation theory and coupled-cluster theory with singles and doubles excitations.

In both series of molecules, the polarizabilities in the directions perpendicular to the long axis of the molecules increase linearly with the size of a molecule, reflecting an increase in the number of electrons in the system. Polarizabilities along the long axis of a molecule increase supralinearly as the length of the molecule increases. This supralinear increase can be understood in terms of increasing $\pi$-electron conjugation that decreases the excitation energy.

For both the neutrals and the cations, the dynamic polarizabilities are always greater than the static polarizabilities. Such increases in polarizability in oscillating fields have important implications for the probabilities of nonadiabatic excitation of these systems in near-IR laser fields. We find that, except in the case of dodecahexene, the dynamic polarizabilities show nonresonant response.

Except for the smallest member in each series (benzene and butadiene), polarizability increases upon ionization (electron removal), and this increase becomes more pronounced with larger molecular size, particularly in the case of dynamic polarizabilities. For example, for octadecanonene and tetracene cations, the relative increases in polarizability along the long axis of the molecule are ∼245%. Such behavior of the polarizabilities of large molecules is qualitatively different from that of small molecules (or atoms), for which polarizabilities decrease upon ionization. This again has significant implications for the mechanism of coupling of such molecules and their nascent ions with the strong near-IR laser field.

For the polyenes, the increase of polarizability upon ionization can be explained in terms of a decrease in the excitation energy when the molecule is ionized. The qualitative trends can be turned into semiquantitative relations between the polarizabilities of the ions and neutrals. By scaling the polarizability of the neutral with the ratio of the first excitation energy of the neutral and the corresponding excitation energy of the ion, we can obtain a very good agreement for the polarizabilities of the polyene cations. Good agreement can also be obtained using the HOMO−LUMO orbital energies. In the polyacenes, the lowest energy states that contribute to the axial polarizability result from a strong interaction between two configurations. Because the weighting of these configurations changes on ionization, it is not possible to use the same scaling relation for the polyacenes.

**Acknowledgment.** This work was supported by grants from the National Science Foundation (CHE 0131157 to H.B.S., CHE 0213483 to R.J.L.) and by the Department of Defense MURI program as managed by the Army Research Office (R.J.L.). We thank the National Center for Supercomputing Applications and ISC at WSU for computer time.

## References and Notes

(1) Joshi, M. P.; Pudavar, H. E.; Swiatkiewicz, J.; Prasad, P. N.; Reianhardt, B. A. *Appl. Phys. Lett.* **1999**, *74*, 170.

(2) Cumpston, B. H.; Ananthavel, S. P.; Barlow, S.; Dyer, D. L.; Ehrlich, J. E.; Erskine, L. L.; Heikal, A. A.; Kuebler, S. M.; Lee, I. Y. S.; McCord-Maughon, D.; Qin, J. Q.; Rockel, H.; Rumi, M.; Wu, X. L.; Marder, S. R.; Perry, J. W. *Nature* **1999**, *398*, 51.

(3) Shen, Y. Z.; Swiatkiewicz, J.; Jakubczyk, D.; Xu, F. M.; Prasad, P. N.; Vaia, R. A.; Reinhardt, B. A. *Appl. Opt.* **2001**, *40*, 938.

(4) Pudavar, H. E.; Joshi, M. P.; Prasad, P. N.; Reinhardt, B. A. *Appl. Phys. Lett.* **1999**, *74*, 1338.

(5) Kawata, S.; Kawata, Y. *Chem. Rev.* **2000**, *100*, 1777.

(6) Fisher, A. M. R.; Murphree, A. L.; Gomer, C. J. *Lasers Surgery Medicine* **1995**, *17*, 2.

(7) Konig, K. *J. Microsco.-Oxford* **2000**, *200*, 83.

(8) Zipfel, W. R.; Williams, R. M.; Christie, R.; Nikitin, A. Y.; Hyman, B. T.; Webb, W. W. *Proc. Natl. Acad. Sci. U.S.A.* **2003**, *100*, 7075.

(9) Rustagi, K. C.; Ducuing, J. *Opt. Commun.* **1974**, *10*, 258.

(10) Agrawal, G. P.; Cojan, C.; Flytzanis, C. *Phys. Rev. B* **1978**, *17*, 776.

(11) Craig, G. S. W.; Cohen, R. E.; Schrock, R. R.; Silbey, R. J.; Puccetti, G.; Ledoux, I.; Zyss, J. *J. Am. Chem. Soc.* **1993**, *115*, 860.

(12) Puccetti, G.; Blancharddesce, M.; Ledoux, I.; Lehn, J. M.; Zyss, J. *J. Phys. Chem.* **1993**, *97*, 9385.

(13) Ward, J. F.; Elliot, D. S. *J. Chem. Phys.* **1978**, *69*, 5438.

(14) Marder, S. R.; Perry, J. W.; Klavetter, F. L.; Grubbs, R. H. *Chem. Mater.* **1989**, *1*, 171.

(15) Tretiak, S.; Mukamel, S. *Chem. Rev.* **2002**, *102*, 3171.

(16) Tretiak, S.; Chernyak, V.; Mukamel, S. *Chem. Phys. Lett.* **1996**, *259*, 55.

(17) Hurst, G. J. B.; Dupuis, M.; Clementi, E. *J. Chem. Phys.* **1988**, *89*, 385.

(18) Kirtman, B.; Toto, J. L.; Robins, K. A.; Hasan, M. *J. Chem. Phys.* **1995**, *102*, 5350.
(19) Balasubramaniam, S.; Applequist, J. *J. Phys. Chem.* **1996**, *100*, 10834.
(20) Tretiak, S.; Chernyak, V.; Mukamel, S. *Phys. Rev. Lett.* **1996**, *77*, 4656.
(21) Schulz, M.; Tretiak, S.; Chernyak, V.; Mukamel, S. *J. Am. Chem. Soc.* **2000**, *122*, 452.
(22) Shanker, B.; Applequist, J. *J. Phys. Chem.* **1996**, *100*, 10834.
(23) Oliveira, L. N.; Amaral, O. A. V.; Castro, M. A.; Fonseca, T. L. *Chem. Phys.* **2003**, *289*, 221.
(24) Lu, Y. J.; Lee, S. L. *Int. J. Quantum. Chem.* **1992**, *44*, 773.
(25) Matsuzawa, N.; Dixon, D. A. *J. Phys. Chem. A* **1992**, *96*, 6241.
(26) Champagne, B.; Mosley, D. H.; Andre, J. M. *J. Chem. Phys.* **1994**, *100*, 2034.
(27) Mukamel, S.; Tretiak, S.; Wagersreiter, T.; Chernyak, V. *Science* **1997**, *277*, 781.
(28) Tretiak, S.; Chernyak, V.; Mukamel, S. *Chem. Phys. Lett.* **1998**, *287*, 75.
(29) Blancharddesce, M.; Lehn, J. M.; Barzoukas, M.; Ledoux, I.; Zyss, J. *Chem. Phys.* **1994**, *181*, 281.
(30) Chen, G. H.; Mukamel, S. *J. Chem. Phys.* **1995**, *103*, 9355.
(31) de Melo, C. P.; Sibley, R. *J. Chem. Phys.* **1988**, *88*, 2558.
(32) Tretiak, S.; Chernyak, V.; Mukamel, S. *J. Chem. Phys.* **1996**, *105*, 8914.
(33) Hurst, G. J. B.; Dupuis, M.; Clementi, E. *J. Chem. Phys.* **1988**, *89*, 385.
(34) Ledoux, I.; Samuel, I. D. W.; Zyss, J.; Yaliraki, S. N.; Schattenmann, F. J.; Schrock, R. R.; Silbey, R. J. *Chem. Phys.* **1999**, *245*, 1.
(35) Hasan, M.; Kim, S. J.; Toto, J. L.; Kirtman, B. *J. Chem. Phys.* **1996**, *105*, 186.
(36) Champagne, B.; Perpete, E. A.; van Gisbergen, S. J. A.; Baerends, E. J.; Snijders, J. G.; Soubra-Ghaoui, C.; Robins, K. A.; Kirtman, B. *J. Chem. Phys.* **1998**, *109*, 10489.
(37) Torrent-Sucarrat, M.; Sola, M.; Duran, M.; Luis, J. M.; Kirtman, B. *J. Chem. Phys.* **2003**, *118*, 711.
(38) Markevitch, A. N.; Smith, S. M.; Romanov, D. A.; Schlegel, H. B.; Ivanov, M. Y.; Levis, R. J. *Phys. Rev. A* **2003**, *68*, Art. No 011402.
(39) Markevitch, A. N.; Romanov, D. A.; Smith, S. M.; Schlegel, H. B.; Ivanov, M. Y.; Levis, R. J. *Phys. Rev. A* **2004**, *69*, Art. No 013401.
(40) Harada, H.; Shimizu, S.; Yatsuhashi, T.; Sakabe, S.; Izawa, Y.; Nakashima, N. *Chem. Phys. Lett.* **2001**, *342*, 563.
(41) Harada, H.; Tanaka, M.; Murakami, M.; Shimizu, S.; Yatsuhashi, T.; Nakashima, N.; Sakabe, S.; Izawa, Y.; Tojo, S.; Majima, T. *J. Phys. Chem. A* **2003**, *107*, 6580.
(42) Lezius, M.; Blanchet, V.; Rayner, D. M.; Villeneuve, D. M.; Stolow, A.; Ivanov, M. Y. *Phys. Rev. Lett.* **2001**, *86*, 51.
(43) Lezius, M.; Blanchet, V.; Ivanov, M. Y.; Stolow, A. *J. Chem. Phys.* **2002**, *117*, 1575.
(44) Delone, N. B.; Krainov, V. P. Chapter 4. In *Atoms in Strong Laser Fields*; Springer-Verlag: Berlin, 1985.
(45) Ammosov, M. V.; Delone, N. B.; Krainov, V. P. *Soviet Physics−JETP* **1986**, *64*, 1191.
(46) Machado, H. J. S.; Hinchliffe, A. *Electron. J. Theor. Chem.* **1997**, *2*, 49.
(47) Craw, J. S.; Hinchliffe, A. *Electron. J. Theor. Chem.* **1996**, *1*, 1.
(48) Frisch, M. J.; Trucks, G. W.; Schlegel, H. B.; Scuseria, G. E.; Robb, M. A.; Cheeseman, J. R.; Montgomery, J. A.; Vreven, T.; Kudin, K. N.; Burant, J. C.; Millam, J. M.; Iyengar, S.; Tomasi, J.; Barone, V.; Mennucci, B.; Cossi, M.; Scalmani, G.; Rega, N.; Petersson, G. A.; Ehara, M.; Toyota, K.; Hada, M.; Fukuda, R.; Hasegawa, J.; Ishida, M.; Nakajima, T.; Kitao, O.; Nakai, H.; Honda, Y.; Nakatsuji, H.; Li, X.; Knox, J. E.; Hratchian, H. P.; Cross, J. B.; Adamo, C.; Jaramillo, J.; Cammi, R.; Pomelli, C.; Gomperts, R.; Stratmann, R. E.; Ochterski, J.; Ayala, P. Y.; Morokuma, K.; Salvador, P.; Dannenberg, J. J.; Zakrzewski, V. G.; Dapprich, S.; Daniels, A. D.; Strain, M. C.; Farkas, Ö.; Malick, D. K.; Rabuck, A. D.; Raghavachari, K.; Foresman, J. B.; Ortiz, J. V.; Cui, Q.; Baboul, A. G.; Clifford, S.; Cioslowski, J.; Stefanov, B. B.; Liu, G.; Liashenko, A.; Piskorz, P.; Komaromi, I.; Martin, R. L.; Fox, D. J.; Keith, T.; Al-Laham, M. A.; Peng, C. Y.; Nanayakkara, A.; Challacombe, M.; Gill, P. M. W.; Johnson, B.; Chen, W.; Wong, M. W.; Andres, J. L.; Gonzalez, C.; Head-Gordon, M.; Replogle, E. S.; Pople, J. A. *Gaussian 01*, Development Version (Revision B.02); Gaussian, Inc.: Pittsburgh, PA, 2002.
(49) Perdew, J. P.; Burke, K.; Ernzerhof, M. *Phys. Rev. Lett.* **1996**, *77*, 3865.
(50) Perdew, J. P.; Burke, K.; Ernzerhof, M. *Phys. Rev. Lett.* **1997**, *78*, 1396.
(51) Frisch, M. J.; Headgordon, M.; Pople, J. A. *Chem. Phys. Lett.* **1990**, *166*, 275.
(52) Frisch, M. J.; Headgordon, M.; Pople, J. A. *Chem. Phys. Lett.* **1990**, *166*, 281.
(53) Head-Gordon, M.; Head-Gordon, T. *Chem. Phys. Lett.* **1994**, *220*, 122.
(54) Head-Gordon, M.; Pople, J. A.; Frisch, M. J. *Chem. Phys. Lett.* **1988**, *153*, 503.
(55) Saebo, S.; Almlof, J. *Chem. Phys. Lett.* **1989**, *154*, 83.
(56) Cizek, J. *Adv. Chem. Phys.* **1969**, *14*, 35.
(57) Purvis, G. D.; Bartlett, R. J. *J. Chem. Phys.* **1982**, *76*, 1910.
(58) Scuseria, G. E.; Janssen, C. L.; Schaefer, H. F., III. *J. Chem. Phys.* **1988**, *89*, 7382.
(59) Scuseria, G. E.; Schaefer, H. F., III. *J. Chem. Phys.* **1989**, *90*, 3629.
(60) Hariharan, P. C.; Pople, J. A. *Chem. Phys. Lett.* **1972**, *66*, 217.
(61) Hehre, W. J.; Ditchfield, R.; Pople, J. A. *J Chem Phys* **1972**, *56*, 2257.
(62) Adamo, C.; Barone, V. *Chem. Phys. Lett.* **1997**, *274*, 242.
(63) Hay, P. J. *J. Chem. Phys.* **1977**, *66*, 4377.
(64) Raghavachari, K.; Trucks, G. W. *J. Chem. Phys.* **1989**, *91*, 1062.
(65) Wachters, A. J. H. *J. Chem. Phys.* **1970**, *52*, 1033.
(66) Rice, J. E.; Handy, N. C. *J. Chem. Phys.* **1991**, *94*, 4959.
(67) Casida, M. E. *Recent Advances in Modern Density Functional Methods*; World Scientific: Singapore, 1995; Vol. 1.
(68) Casida, M. E. *Recent Development and Applications of Modern Density Functional Theory*, *Theoretical and Computational Chemistry*; Elsevier: Amsterdam, 1996; Vol. 4.
(69) Gross, E. K. U.; Kohn, W. *Adv. Quantum Chem.* **1990**, *21*, 255.
(70) Stratmann, R. E.; Scuseria, G. E.; Frisch, M. J. *J. Chem. Phys.* **1998**, *109*, 8218.
(71) van Leeuwen, R. *Phys. Rev. Lett.* **1998**, *80*, 1280.
(72) Adamo, C.; Cossi, M.; Scalmani, G.; Barone, V. *Chem. Phys. Lett.* **1999**, *307*, 265.
(73) Adamo, C.; Scuseria, G. E.; Barone, V. *J. Chem. Phys.* **1999**, *111*, 2889.
(74) Van Caillie, C.; Amos, R. D. *Chem. Phys. Lett.* **2000**, *328*, 446.
(75) van Gisbergen, S. J. A.; Schipper, P. R. T.; Gritsenko, O. V.; Baerends, E. J.; Snijders, J.; Champagne, B.; Kirtman, B. *Phys. Rev. Lett.* **1999**, *83*, 694.
(76) van Faassen, M.; de Boeij, P. L.; van Leeuwen, R.; Berger, J.; Snijders, J. *Phys. Rev. Lett.* **2002**, *88*, 186401.
(77) van Faassen, M.; de Boeij, P. L.; van Leeuwen, R.; Berger, J.; Snijders, J. *J. Chem. Phys.* **2003**, *118*, 1044.
(78) Maroulis, G.; Makris, C.; Hohm, U.; Wachsmuth, U. *J. Phys. Chem. A* **1999**, *103*, 4359.
(79) Sadlej, A. J. *Collect. Czech. Chem. Commun.* **1988**, *53*, 1995.
(80) Almlof, J.; Taylor, P. R. *J. Chem. Phys.* **1990**, *92*, 551.
(81) Bishop, D. M.; Maroulis, G. J. *J. Chem. Phys.* **1985**, *82*, 2380.
(82) Davidson, E. R.; Feller, D. *Chem. Rev.* **1986**, *86*, 681.
(83) Spackman, M. A. *J. Phys. Chem.* **1989**, *93*, 7594.
(84) Van Duijneveldt-Van de Rijdt, J. G. C. M.; Van Duijneveldt, F. B. *J. Mol. Struct.* **1982**, *89*, 185.
(85) Hohm, U.; Trumper, U. *Ber. Bunsen-Ges. Phys. Chem.* **1992**, *96*, 1061.
(86) Shanker, B.; Applequist, J. *J. Chem. Phys.* **1996**, *104*, 6109.
(87) Tretiak, S.; Chernyak, V.; Mukamel, S. *Phys. Rev. Lett.* **1996**, *77*, 4656.
(88) Tretiak, S.; Mukamel, S. *Chem. Rev.* **2002**, *102*, 3171.
(89) Ward, J. F.; Elliot, D. S. *J. Chem. Phys.* **1978**, *69*, 5438.
(90) Tretiak, S.; Chernyak, V.; Mukamel, S. *Chem. Phys. Lett* **1998**, *287*, 75.
(91) Kavanaugh, T.; Silbey, R. J. *J. Chem. Phys.* **1991**, *95*, 6924.
(92) Hankin, S. M.; Villeneuve, D. M.; Corkum, P. B.; Rayner, D. M. *Phys. Rev. Lett.* **2000**, *84*, 5082.
(93) Hankin, S. M.; Villeneuve, D. M.; Corkum, P. B.; Rayner, D. M. *Phys. Rev. A* **2001**, *6401*, 3405.
(94) DeWitt, M. J.; Levis, R. J. *Phys. Rev. Lett.* **1998**, *81*, 5101.
(95) Levis, R. J.; DeWitt, M. J. *J. Phys. Chem. A* **1999**, *103*, 6493.
(96) Markevitch, A. N.; Romanov, D. A.; Smith, S. M.; Levis, R. J. *Phys. Rev. Lett.* **2004**, *92*.
(97) Ward, R. F.; Sturrus, W. G.; Lundeen, S. R. *Phys. Rev. A* **1996**, *53*, 113.
(98) Cotton, F. A. *Chemical Applications of Group Theory*, 3rd ed.; John Wiley & Sons: New York, 1990.
(99) Castillejo, M.; Couris, S.; Koudoumas, E.; Martin, M. *Chem. Phys. Lett.* **1999**, *308*, 373.
(100) Itakura, R.; Watanabe, J.; Hishikawa, A.; Yamanouchi, K. *J. Chem. Phys.* **2001**, *114*, 5598.